Ultrasound in Med. & Biol., Vol. 29, No. 11, pp. 1625–1634, 2003

0301-5629/03/$–see front matter

ELSEVIER

doi:10.1016/j.ultrasmedbio.2003.08.002

● *Original Contribution*

THRESHOLD ESTIMATES AND SUPERTHRESHOLD BEHAVIOR OF ULTRASOUND-INDUCED LUNG HEMORRHAGE IN ADULT RATS: ROLE OF PULSE DURATION

WILLIAM D. O'BRIEN, JR.,* DOUGLAS G. SIMPSON,‡ LEON A. FRIZZELL* and JAMES F. ZACHARY†

*Bioacoustics Research Laboratory, Department of Electrical and Computer Engineering and †Department of Veterinary Pathobiology, University of Illinois, Urbana, IL, USA; and ‡Department of Statistics, University of Illinois, Champaign, IL, USA

(*Received* 14 *March* 2003; *revised* 27 *July* 2003; *in final form* 8 *August* 2003)

Abstract—The study objective was to estimate the pressure threshold (ED_{05}, effective dose, or *in situ* peak rarefactional pressure associated with 5% probability of lesions) of ultrasound (US)-induced lung hemorrhage as a function of pulse duration (PD) in adult rats. A total of 220 10- to 11-week-old 250-g female Sprague-Dawley rats (Harlan) were randomly divided into 20 ultrasonic exposure groups (10 rats/group) and one sham group (20 rats). The 20 ultrasonic exposure groups (2.8-MHz; 10-s exposure duration; 1-kHz PRF; −6-dB pulse-echo focal beam width of 470 μm) were divided into four PD groups (1.3, 4.4, 8.2 and 11.6 μs) and, for each PD group, there were five *in situ* peak rarefactional pressures (range between 4 and 9 MPa). Rats were weighed, anesthetized, depilated, exposed, and euthanized under anesthesia. The left lung was removed and scored for the occurrence of hemorrhage. If hemorrhage was present, the lesion surface area and depth were measured. Individuals involved in animal handling, exposure and lesion scoring were "blinded" to the exposure conditions. Logistic regression analysis was used to examine the dependence of the lesion occurrences, and Gaussian tobit regression analysis was used to examine the dependence of the lesion surface areas and depths on *in situ* peak rarefactional pressure and PD. Threshold results are reported in terms of ED_{05}. For PDs of 1.3, 4.4, 8.2 and 11.6 μs, respectively, lesion occurrence ED_{05}s were 3.1, 2.8, 2.3 and 2.0 MPa with standard errors around 0.6 MPa. Lesion size ED_{05}s showed similar values. A mechanical index (MI) of 1.9, the US Food and Drug Administration (FDA) regulatory limit of diagnostic US equipment, is equivalent to the adult rat's *in situ* peak rarefactional pressure of 4.0 MPa. PDs of 8.2 and 11.6 μs had ED_{05}s more than 2 standard errors below 4.0 MPa, indicating that the ED_{05}s of these two PDs are statistically significantly different from 4.0 MPa. The ED_{05} threshold levels for a PD of 1.3 μs are consistent with previous US-induced lung hemorrhage studies. As the PD increases, the ED_{05} levels decrease, suggesting greater likelihood of lung damage as the PD increases. All of the ED_{05}s are less than the FDA limit. (E-mail: wdo@uiuc.edu)

Key Words: **Ultrasound bioeffects, Rat lung, Pulsed ultrasound, Lung hemorrhage, Pulse duration.**

INTRODUCTION

The effect of exposure timing quantities (*e.g.*, pulse duration or PD, exposure duration or ED, total on-time, and pulse repetition frequency or PRF) on the threshold for ultrasound (US)-induced lung hemorrhage and on the size of the lesions at superthreshold levels has been examined to a limited extent (Child et al. 1990). Our study examined the role of PD in producing US-induced lung hemorrhage when PRF and ED were held constant. Specifically, the threshold estimates and superthreshold behavior of US-induced lung hemorrhage in adult rats were examined at four pulse durations. Pulse duration is the on-time (time duration) of an individual ultrasonic pulse, typically in the range of 1 μs for diagnostic US equipment.

There appears to be only one study that has reported a dependency of US-induced lung hemorrhage on pulse duration (Child et al. 1990); even though pulse duration is an important quantity that is varied by diagnostic US equipment. However, there have been numerous studies that have demonstrated that US-induced lung hemorrhage can occur in mice, rats, rabbits, monkeys and pigs (AIUM 2000; Child et al. 1990; Hartman et al. 1990;

Address correspondence to: William D. O'Brien, Jr., Bioacoustics Research Laboratory, Department of Electrical and Computer Engineering, University of Illinois, 405 North Mathews, Urbana, IL 61801 USA. E-mail: wdo@uiuc.edu

Penney et al. 1993; Raeman et al. 1993, 1996; Frizzell et al. 1994, 2003; Tarental and Canfield 1994; Zachary and O'Brien 1995; Baggs et al. 1996; Holland et al. 1996; O'Brien and Zachary 1997; Dalecki et al. 1997a, 1997b; O'Brien et al. 2000, 2001a, 2001b, 2002, 2003; Zachary et al. 2001a, 2001b; Kramer et al. 2001).

The pressure threshold for lung hemorrhage in mice has been reported to be dependent on pulse duration (Child et al. 1990). At an ultrasonic frequency of 3.7 MHz, the peak rarefactional pressure threshold was 1.4 MPa for a PD of 1 μs, whereas the threshold was 1.0 MPa for a PD of 10 μs. The exposure duration (ED, 180 s) and duty cycle (0.1%) were the same, so the PRF was different by a factor of 10 (100 vs. 1000 Hz). Also, in the same study, but at a different frequency (1.2 MHz), when the PD (10 μs) and ED (180 s) were held constant, the same peak rarefactional pressure threshold (0.7 MPa) was observed, even though the PRF and, hence, the duty cycle or number of pulses, was varied (10 vs. 100 Hz). Thus, while the principal goal of the study by Child et al. (1990) was not aimed at assessing the dependency of US-induced lung hemorrhage on PD, its observations strongly suggested that PD influenced the pressure threshold value.

Therefore, a directed study focused on whether or not US-induced lung hemorrhage is influenced by pulse duration was warranted. In addition to estimating the threshold as a function of PD, this study also examined the superthreshold behavior as a function of PD.

MATERIALS AND METHODS

Exposimetry

The exposimetry and calibration procedures have been described previously in detail (Zachary et al. 2001a). Ultrasonic exposures were conducted using one focused, 19-mm diameter, lithium niobate ultrasonic transducer (Valpey Fisher, Hopkinton, MA). Water-based (highly degassed water, 22°C) pulse-echo ultrasonic field distribution measurements were performed according to established procedures (Raum and O'Brien 1997) and yielded a center frequency of 2.8 MHz, a fractional band width of 12%, a focal length of 19 mm, a −6-dB focal beam width of 470 μm, and a −6-dB depth of focus of 2.7 mm.

An automated procedure was developed to routinely calibrate the US fields (Sempsrott and O'Brien 1999; Zachary et al. 2001a) that was based on established standards (AIUM/NEMA 1998a, 1998b). The source transducer was mounted in a water tank (highly degassed water, 22°C) and its drive voltage was supplied by a RAM5000 (Ritec, Inc., Warwick, RI). A calibrated polyvinylidene difluoride (PVDF) membrane hydrophones (Marconi Model Y-34–6543, Chelmsford, UK) was mounted to the computer-controlled micropositioning (linear accuracy: 2 μm) system (Daedal, Inc., Harrisburg, PA). The hydrophone's signal was digitized with an oscilloscope (500 Ms/s, LeCroy Model 9354TM, Chestnut Ridge, NY), and transferred to the same computer (Dell Pentium II) that controlled the positioning system. Off-line processing (Matlab®, The Mathworks, Natick, MA) yielded the peak water-based rarefactional pressure $p_{r(\text{in vitro})}$ and the peak water-based compressional pressure $p_{c(\text{in vitro})}$.

A total of 25 independent water-based calibrations of the 2.8-MHz transducer were conducted before, during, and after the 5-month period of the experiments. At the exposure levels used in this study, the relative SD (SD × 100/mean) was 17% for $p_{r(\text{in vitro})}$ and 20% for $p_{c(\text{in vitro})}$.

The *in situ* (at the pleural surface) peak rarefactional and compressional pressures (Table 1) were estimated, as has been done in previous studies (O'Brien et al. 2000, 2001a, 2001b, 2002, 2003; Zachary et al. 2001a, 2001b; Kramer et al. 2001), for each rat from

$$p_{r(\text{in situ})} = p_{r(\text{in vitro})} e^{-(A \cdot x)}, \quad (1)$$

and

$$p_{c(\text{in situ})} = p_{c(\text{in vitro})} e^{-(A \cdot x)}. \quad (2)$$

The mean attenuation coefficient, A, of the rat intercostal tissue used herein was determined from independent studies where, at 2.8 MHz, A = 2.8 dB/cm = 0.32 Np/cm (Teotico et al. 2001; Towa et al. 2002). The measured intercostal tissue thicknesses, x, were used in eqns (1) and (2) to calculate $p_{r(\text{in situ})}$ and $p_{c(\text{in situ})}$.

The distance between the transducer and the rat lung surface did not vary by more than 1 mm; the lung surface location was monitored *via* the pulse-echo capability of the RAM5000 system. The −6-dB depth of focus was 2.7 mm, so the lung surface remained within the focal region as a function of the animal's breathing. Also, the orientation of the chest wall surface did not visually change as a function of breathing. Because the chest wall surface and the lung surface track each other, the orientation between the beam axis and the pleural surface did not change. In addition, the center-to-center rib spacing of rats is about 5 mm (Zachary et al. 2001a); with a beam width at the pleural surface of 470 μm, there was adequate space between the ribs for the sound field. Therefore, the observations and findings reported herein are not believed to be a function of lung surface or rib orientation, position or movement relative to the ultrasonic field.

Table 1. Mean values of the *in situ* (at the pleural surface) peak rarefactional pressure $p_{r(\text{in situ})}$ and peak compressional pressure $p_{c(\text{in situ})}$.

n of animals	$p_{r(\text{in situ})}$, (MPa)	$p_{c(\text{in situ})}$, (MPa)	MI	% lesions (uncertainty)	Mean (SEM) lesion area (mm^2)	Mean (SEM) lesion depth (mm)
Pulse duration = 1.3 μs						
10	4.2	4.5	2.3	10 (9)	0.025 (0.025)	0.020 (0.020)
10	5.1	5.6	2.8	20 (13)	0.23 (0.15)	0.13 (0.10)
10	6.0	6.7	3.3	30 (14)	1.50 (0.83)	0.37 (0.19)
10	6.9	7.8	3.8	50 (16)	0.49 (0.22)	0.28 (0.13)
10	7.7	8.9	4.2	70 (14)	2.18 (0.81)	0.79 (0.28)
Pulse duration = 4.4 μs						
10	4.1	4.6	2.3	10 (9)	0.23 (0.23)	0.17 (0.17)
10	5.3	6.2	2.9	30 (14)	0.36 (0.22)	0.32 (0.21)
10	6.4	7.8	3.5	60 (15)	2.08 (1.01)	0.89 (0.37)
10	7.5	9.3	4.1	70 (14)	5.81 (2.08)	1.45 (0.42)
10	8.7	11	4.8	90 (9)	7.35 (2.58)	1.35 (0.30)
Pulse duration = 8.2 μs						
10	4.0	4.1	2.2	0 (0)	0 (0)	0 (0)
10	5.1	5.8	2.8	60 (15)	1.11 (0.45)	0.49 (0.18)
10	6.4	7.7	3.5	70 (15)	4.40 (1.88)	1.31 (0.43)
10	7.6	9.5	4.2	90 (9)	7.06 (1.70)	1.97 (0.40)
10	8.1	11	4.8	80 (13)	6.94 (1.89)	1.93 (0.49)
Pulse duration = 11.6 μs						
10	3.9	4.1	2.1	10 (9)	0.072 (0.072)	0.073 (0.073)
10	5.1	5.8	2.8	60 (15)	0.97 (0.40)	0.53 (0.21)
10	6.3	7.5	3.4	40 (15)	1.80 (0.81)	0.77 (0.34)
10	7.5	9.2	4.1	100 (0)	8.27 (1.78)	2.36 (0.36)
10	8.7	11	4.8	80 (13)	5.94 (1.82)	1.82 (0.40)

All rats were exposed to pulsed US (PRF = 1 kHz and ED = 10 s). The 20 sham rats had no lesions and were exposed at a PRF of 10 Hz ($p_{r(\text{in situ})}$ = 0.26 MPa; $p_{c(\text{in situ})}$ = 0.31 MPa; MI = 0.15). Mean values of the MI, as measured according to the applicable standard (AIUM/NEMA 1998b), are provided because the MI is a regulated quantity of diagnostic US equipment.

The mechanical index (MI) was determined (AIUM/NEMA 1998b) from:

$$MI = \frac{p_{r.3}}{\sqrt{f}}, \tag{3}$$

where $p_{r.3}$ (in MPa) is the water-based peak rarefactional pressure derated by 0.3 dB/cm-MHz at the location where the derated pulse intensity integral is a maximum, and where f is the ultrasonic frequency (in MHz). The MI is reported because it is a regulated quantity (FDA 1997) of diagnostic US systems, and its value is available to system operators. Thus, there is value to provide the MI for each of our exposure settings to give general guidance to manufacturers and operators as to the levels we used in this study. Further, it is a quantity that cannot be determined from $p_{r(\text{in situ})}$, the *in situ* (at the pleural surface) peak rarefactional pressure used herein to report our findings; therefore, the calculated MI for each of the exposure conditions is listed (Table 1) so that the reader can see how the MI is related to each of the *in situ* pressure values.

Animals

The experimental protocol was approved by the Laboratory Animal Care Advisory Committee at the University of Illinois at Urbana-Champaign and satisfied all campus and National Institutes of Health (NIH) rules for the humane use of laboratory animals. Rats were housed in an Association for Assessment and Accreditation of Laboratory Animal Care (AAALAC)-approved animal facility, placed in groups of 1 to 3 in polycarbonate cages with β-chip bedding and wire bar lids, and provided food and water *ad lib*. AAALAC (Rockville, MD) is a private nonprofit organization that promotes the humane treatment of animals in science through a voluntary accreditation program.

A total of 220 10- to 11-week-old 250 $\pm$ 12 g (mean $\pm$ SD) female Sprague-Dawley rats (Harlan Sprague Dawley Laboratories, Indianapolis, IN) were randomly divided into 20 ultrasonic exposure groups (10 rats per group) and one sham group (20 rats); no lesions were produced in the sham group. The 20 ultrasonic exposure groups were divided into four PD groups, and for each PD group, there were five *in situ* peak rarefactional pressures. Each of the four PD groups were designed to have the same five *in situ* peak rarefactional pressures (4.1, 5.3, 6.5, 7.7 and 8.9 MPa). The design was based on previous studies (O'Brien et al. 2001a, 2001b; Zachary et al. 2001a, 2001b). Because the chest wall thicknesses were not the same as the thickness used to design the study, and a design error occurred in determining the

$p_{r(\text{in vitro})}$ levels for the 1.3-μs PD, the estimated *in situ* peak rarefactional pressures obtained herein were slightly different (Table 1). The individuals involved in animal handling, exposure and lesion scoring were "blinded" to the exposure condition. The exposure conditions for each animal were revealed only after the final results were tabulated.

The rat exposure and analysis procedures have been described previously in detail (Kramer et al. 2001; O'Brien et al. 2001a, 2001b, 2002; Zachary et al. 2001a; Frizzell et al. 2003). Rats were weighed and then anesthetized with ketamine hydrochloride (87.0 mg/kg) and xylazine (13.0 mg/kg) administered IP. Hair of the left thorax was removed with an electric clipper, followed by a depilatory agent (Nair®, Carter-Wallace, Inc., New York, NY) to maximize sound transmission. A black dot was placed at approximately the sixth to ninth rib to guide the positioning of the ultrasonic beam. Anesthetized animals were placed in a specially designed transducer holder. A removable pointer, attached to the transducer, was used to position the ultrasonic beam perpendicular to the skin at the position of the black dot with the beam focal region approximately at the lung surface. The holder with animal and mounted transducer were placed in highly degassed, temperature-controlled (30°C) water. The low-power pulse-echo RAM5000 signal (see sham exposures, Table 1) was displayed on an oscilloscope and used to adjust the axial center of the focal region to within 1 mm of the lung surface. The ultrasonically exposed animals received the *in situ* peak rarefactional pressure and PDs indicated in Table 1. Exposure duration (10 s) and PRF (1 kHz) were the same for each animal exposure. Following exposure, animals were removed from the water and holder, and then euthanized under anesthesia by cervical dislocation.

The thorax was opened and the thickness of each left thoracic wall (skin, rib cage, and parietal pleura) was measured using a digital micrometer (accuracy: 10 μm; Mitutoyo Corp., Kawasaki, Kanagawa, Japan) to calculate $p_{r(\text{in situ})}$. The left lung lobe was scored for the presence or absence of hemorrhage and then fixed by immersion in 10% neutral-buffered formalin for a minimum of 24 h. After fixation, the elliptical dimensions of each lung lesion at the visceral pleural surface were measured using a digital micrometer, where "a" is the semimajor axis and "b" is the semiminor axis. The lesion was then bisected and the depth "d" of the lesion within the pulmonary parenchyma was also measured. The surface area (πab) and volume (πabd/3) of the lesion were calculated for each animal. Each half of the bisected lesion was embedded in paraffin, sectioned at 5 μm, stained with hematoxylin and eosin and evaluated microscopically.

Table 2. Summary of logistic regression model for occurrence of lesions in 200 rats

Variable	Coefficient	SE	*z* value	*p* value*
Intercept	−5.663	0.859	−6.59	<0.0001
$p_{r(\text{in situ})}$	0.828	0.125	6.63	<0.0001
PD	0.0954	0.0436	2.19	0.029

*Observed significance level of test that the coefficient equals zero.

Statistics

Logistic regression analysis was used to examine the dependence of the lesion incidence rates on *in situ* peak rarefactional pressure, $p_{r(\text{in situ})}$ and PD. The logistic regression analysis models the log-odds of an event (*i.e.*, occurrence of a lesion) as a linear function with coefficients for each of the variables in the study (Agresti 1996). If P denotes the probability of a lesion, then the logistic regression model has the form:

$$\log\left(\frac{P}{1-P}\right) = (\text{Coef}_1)(\text{Var}_1) + (\text{Coef}_2)(\text{Var}_2) + \ldots + (\text{Coef}_k)(\text{Var}_k), \quad (4)$$

where Var_i denotes a variable in the model and Coef_i denotes the corresponding coefficient, which is estimated from the data (Table 2). Logistic regression was performed using the S-Plus® (Insightful Corp., Seattle, WA) function, *glm*. The initial model included $p_{r(\text{in situ})}$, PD and the interaction between $p_{r(\text{in situ})}$ and PD. If the interaction was not significant, then only the main effects were included in the model. Logistic regression estimates were transformed to yield estimates and confidence intervals for two effective dose levels, the ED_{05} and ED_{50} levels (*i.e.*, the *in situ* peak rarefactional pressure associated with 5% and 50% probabilities of lesions, respectively) (Simpson et al. 1996; Zachary et al. 2001a). It is understood that *in situ* peak rarefactional pressure is a dose in the generalized sense of an exposure quantity rather than in the specific sense of a chemical concentration or radiation dose. Generally, for safety studies, the threshold is set at a relatively low probability, such as 5%, whereas, for mechanism studies, a higher threshold such as 50% may be appropriate. Used herein, the ED_{05} is the threshold level.

Depth and root surface area ($\sqrt{}$surface area) of lesions were analyzed using Gaussian tobit regression using the S-Plus® *survReg* function. The tobit regression model includes a threshold for the occurrence of observations equal to zero, and a linear regression model for observations greater than zero (Amemiya 1984; Billard 1994). In particular, let Z denote a Normally distributed random variable with mean E(Z) and standard deviation S, where

$$E(Z) = (\text{Coef}_1)(\text{Var}_1) + (\text{Coef}_2)(\text{Var}_2) + \ldots + (\text{Coef}_k)(\text{Var}_k). \quad (5)$$

Let $Y = Z$ if $Z > 0$ and $Y = 0$ if $Z \leq 0$. Then Y follows a tobit regression model; it has a normal distribution truncated below at zero. An important feature of the tobit model is that it allows for a positive probability of zero, which, in the analysis of US-induced lesions, corresponds to a lung with no lesions (lesion depth and size = 0). The probability of lesion occurrence is equal to the probability that the depth and surface area are strictly greater than zero. In the tobit model, the probability P of a strictly positive observation satisfies the equation:

$$S \cdot Q(P) = (\text{Coef}_1)(\text{Var}_1) + (\text{Coef}_2)(\text{Var}_2) + \ldots + (\text{Coef}_k)(\text{Var}_k) \quad (6)$$

where $Q(P)$ is the 100Pth percentile of the standard normal distribution which, except for the scale S, is the same form as in probit regression (Agresti 1996). If the right side of eqn (5) is positive, then it is also the conditional median of Y, given Var_1, Var_2, ..., Var_k (Galfalvy and Simpson 1999).

For animals with lesions, the depth or root surface area was included as the response measurement. For animals without lesions, the depth or root surface area was included as a zero value. Graphs of ordered residuals vs. normal percentiles indicated the need for a square root transformation of surface area to achieve an adequate fit of a linear tobit model. The ED_{05} and ED_{50} were determined by solving eqn (6) for the values of $p_{r(\text{in situ})}$ such that $p = 0.05$ and $p = 0.50$, respectively. These were the exposure levels so that the estimated probability of a lesion of positive size equaled 5% and 50%, respectively. For example, the ED_{05} for lesion depth was the *in situ* peak rarefactional pressure, so that only 5% of exposed lungs are expected to exhibit lesions with positive depth. Standard errors for these quantities were obtained by first-order Taylor series approximations. Standard errors and confidence intervals were computed in S-Plus® using matrix calculations. The 95% confidence intervals were computed as (estimate) ± (1.96) * (standard error).

RESULTS

Chest wall thickness

The chest wall thickness over the left lung was measured. The mean ± SD (range) values of the chest wall thicknesses were: 4.3 ± 0.19 (3.7 to 4.7) mm (n = 200, for the exposed animals).

Results for lesion incidence

The logistic regression model for occurrence of lesions (Fig. 1a) was highly statistically significant: the likelihood ratio chi-square for the model was 65.76 on two degrees of freedom, with a p value of less than 0.0001. This is strong evidence of a PD and/or $p_{r(\text{in situ})}$ effect. The interaction between PD and $p_{r(\text{in situ})}$ was not significant.

Table 2 gives the coefficient estimates, standard errors (SE) and z-values (estimate/SE) for each term in the model. A z-value whose absolute value exceeds 1.96 is statistically significant at level 0.05. The interaction between PD and $p_{r(\text{in situ})}$ was not significant. Both main effect variables were statistically significant at level 0.05: 1. $p_{r(\text{in situ})}$, in MPa; and 2. PD, in μs. The coefficient for $p_{r(\text{in situ})}$ is the increase in log-odds of a lesion for each 1-MPa increase in $p_{r(\text{in situ})}$. Similarly, the coefficient for PD is the increase in log-odds of a lesion for each 1-μs increase in PD.

Table 3 gives ED_{05} thresholds and ED_{50} estimates for occurrence of lesions at the 4 levels of PD: 1.3, 4.4, 8.2 and 11.6 μs. Also included are SE of the estimates. The 95% confidence intervals (estimate ± 1.96 SE) for the ED_{05} all overlap, indicating that there is considerable uncertainty in estimating the ED_{05} difference despite the statistical significance of the pulse duration effect. The ED_{50} values are estimated with greater precision, and the 95% confidence intervals for the two most extreme pulse durations (1.3 and 11.6 μs) are nonoverlapping. Because the PD coefficient in the model is statistically significant, the upward trend in the occurrence probability of a lesion as the pulse duration increases is significant, despite the uncertainty in estimating the thresholds.

Results for lesion depth

The tobit regression model for lesion depth (Fig. 1b) was highly statistically significant: the likelihood ratio chi-square for the model was 90.02 on two degrees of freedom, with a p value of less than 0.0001. This is strong evidence of a PD and/or $p_{r(\text{in situ})}$ effect. The interaction between PD and $p_{r(\text{in situ})}$ was not significant. Table 4 gives the main effect coefficient estimates for PD and $p_{r(\text{in situ})}$. Both were statistically significant at level 0.05. The estimated log(scale) refers to the natural logarithm of the error SD S of eqn (5).

Table 3 gives ED_{05} thresholds and ED_{50} estimates derived from the tobit regression of depth. The trend in the estimates is clear, although the four 95% ED_{05} confidence intervals overlap. The two most extreme ED_{50} confidence intervals, corresponding to pulse durations of 1.3 μs and 11.6 μs, are nonoverlapping. The significance of the PD coefficient in the tobit model indicates that the upward trend in lesion depth with increasing PD is statistically signficant.

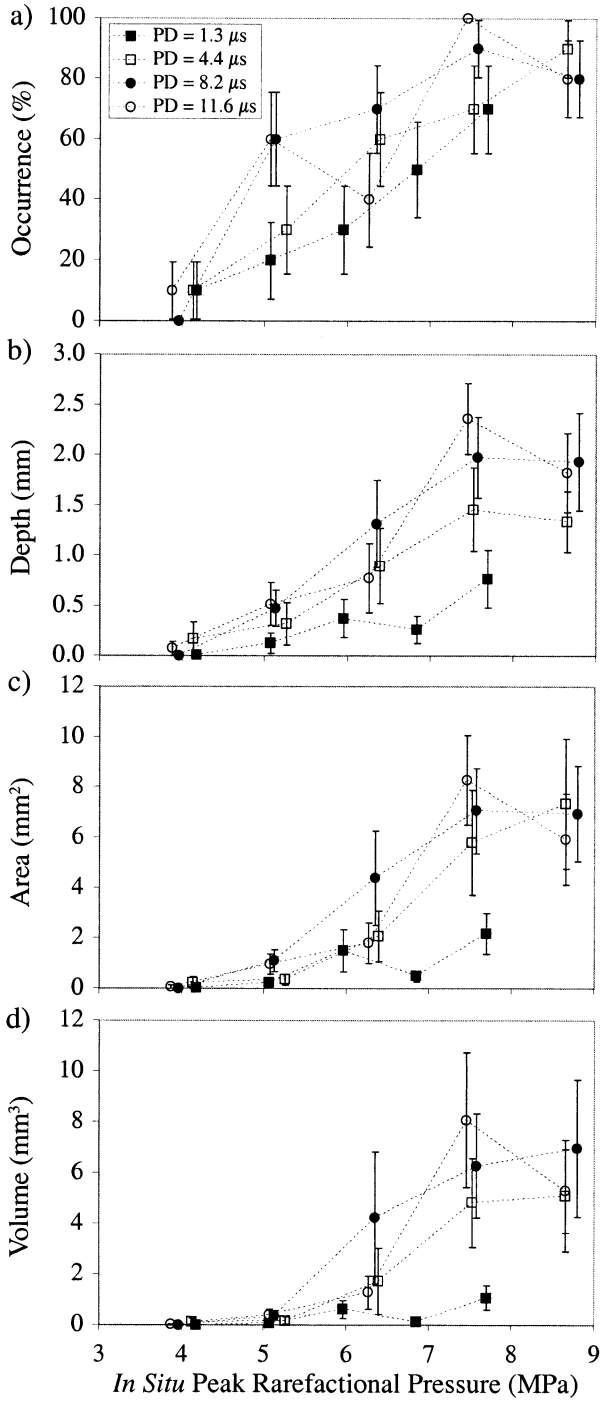

Fig. 1. (a) Lesion occurrence, (b) lesion depth, (c) lesion surface area, and (d) lesion surface volume as a function of the *in situ* peak rarefactional pressure for four PDs. The dashed lines are straight lines connecting the mean values, intended to provide graphical guidance for the four PD exposures. Error bars are the SE of the mean (n = 10 for each exposure condition).

Table 3. ED_{05} and ED_{50} threshold estimates for occurrence, depth and surface area of lesions in 200 rats

		Threshold* (MPa)	
Endpoint	PD (μs)	ED_{05} (SE)	ED_{50} (SE)
Occurrence	1.3	3.13 (± 0.58)	6.69 (± 0.33)
	4.4	2.77 (± 0.56)	6.33 (± 0.22)
	8.2	2.34 (± 0.60)	5.89 (± 0.23)
	11.6	1.95 (± 0.69)	5.50 (± 0.35)
Depth	1.3	3.45 (± 0.45)	6.82 (± 0.30)
	4.4	2.97 (± 0.45)	6.35 (± 0.21)
	8.2	2.39 (± 0.50)	5.77 (± 0.22)
	11.6	1.87 (± 0.60)	5.25 (± 0.33)
Area	1.3	3.29 (± 0.43)	6.48 (± 0.28)
	4.4	2.93 (± 0.42)	6.12 (± 0.21)
	8.2	2.48 (± 0.47)	5.68 (± 0.22)
	11.6	2.09 (± 0.55)	5.28 (± 0.30)

*ED_{05} = obtained by inverting the logistic regression model for the 5% probability or the tobit model for 95% censoring at zero; ED_{50} = obtained by inverting the logistic regression model for the 50% probability or the tobit model for 50% censoring at zero.

Results for lesion surface area

The tobit regression model for lesion surface area (Fig. 1c) was highly statistically significant: the likelihood ratio chi-square for the model was 93.92 on two degrees of freedom, with a p value of less than 0.0001. This is strong evidence of a PD and/or $p_{r(\text{in situ})}$ effect. The interaction between PD and $p_{r(\text{in situ})}$ was not significant. Table 5 gives the main effect coefficient estimates for PD and $p_{r(\text{in situ})}$. Both were statistically significant at level 0.05. The significance of the PD coefficient indicates that increases in PD are associated with increases in lesion surface area. The estimated log(scale) refers to the logarithm of the error SD S of eqn (5).

Table 3 gives ED_{05} thresholds and ED_{50} estimates derived from the tobit regression of area. The results are similar to the results for lesion depth. There is a clear trend in the estimates, but the 95% confidence intervals for ED_{05} overlap due to the uncertainty in estimating ED_{05} from these data. The two most extreme ED_{50} confidence intervals, corresponding to PDs of 1.3 μs and 11.6 μs, are nonoverlapping.

Lesion volume was not evaluated statistically be-

Table 4. Summary of Gaussian tobit model for depth of lesions in 200 rats

Variable	Coefficient	SE	z value	p value*
Intercept	−4.972	0.611	−8.14	<0.0001
$p_{r(\text{in situ})}$	0.708	0.0824	8.59	<0.0001
PD	0.108	0.0307	3.53	0.0004
Log(scale)	0.374	0.0752	4.97	<0.0001

*Observed significance level of test that the coefficient equals zero.

Table 5. Summary of Gaussian tobit model for square root surface areas of lesions in 200 rats

Variable	Coefficient	SE	*z* value	*p* value*
Intercept	−5.619	0.687	−8.18	<0.0001
$p_{r(\text{in situ})}$	0.847	0.0932	9.09	<0.0001
PD	0.099	0.0345	2.86	0.0042
Log(scale)	0.498	0.0762	6.53	<0.0001

*Observed significance level of test that the coefficient equals zero.

cause it is not an independent variable, but is provided graphically (Fig. 1d) for completeness. The consistency of model results across lesion occurrence, depth and surface area is evidence for the appropriateness of the logistic and tobit regression models for the data.

DISCUSSION

The main purpose of this study was to estimate the pressure threshold (ED_{05}) of US-induced lung damage as a function of PD in adult rats. This purpose was accomplished by experimentally determining exposure-effect dependencies (Fig. 1). These exposure-effect dependencies also allowed us to quantify the superthreshold behavior of US-induced lung hemorrhage using the ED_{50} estimate.

As indicated by the significance of the PD coefficients, there were statistically significant trends in the probability, depth and surface area of lesions as PD increased. These upward trends in probability and size of lesions translate into downward trends in the ED_{05} and ED_{50} thresholds as PD increases (Fig. 2). However, for lesion occurrence, depth and surface area, the four ED_{05} threshold values were not statistically significantly different. It is conjectured that the ED_{05} thresholds are at the boundaries of the experimental levels and, thus, estimated with considerable uncertainty compared with the trends in occurrence, depth and surface area within the experimental range. The same decreasing trend was noted for the MI thresholds (Fig. 3). The MI thresholds (1.5, 1.3, 1.1 and 0.9) were based on the ED_{05} occurrence thresholds (3.1, 2.8, 2.3 and 2.0 MPa, respectively) so this trend is also significant. Note that all of the MI threshold values are less than 1.9, the FDA regulatory limit (FDA 1997) for the study reported herein. An MI of 1.9 is equivalent to the adult rat's *in situ* peak rarefactional pressure of 4.0 MPa.

Likewise, there were decreasing ED_{50} superthreshold estimate trends noted for lesion occurrence, depth and surface area as the PD increased (Fig. 4). For lesion occurrence, depth and surface area, the two most extreme ED_{50} values (PDs of 1.3 μs and 11.6 μs)

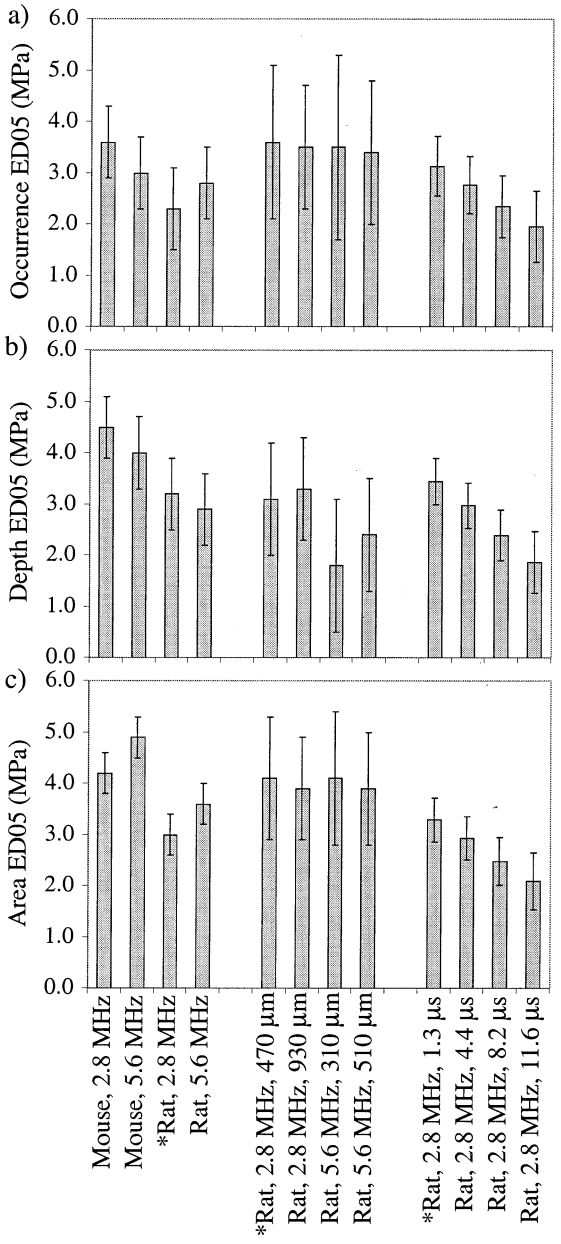

Fig. 2. The (a) lesion ED_{05} threshold occurrence, (b) lesion ED_{05} threshold depth, and (c) lesion ED_{05} threshold surface area in this study (right set of 4 bars) compared with two previous studies (left set of 4 bars, Zachary et al. 2001b; middle set of 4 bars, O'Brien et al. 2001a).

were significant, suggesting that increasing PD decreased the ED_{50} estimate.

What is particularly interesting is that, although there was an almost 10-fold increase in the temporal-average US exposure level as the PD increased from 1.3 μs to 11.6 μs, the four ED_{05} occurrence and size thresholds were not significantly different, although

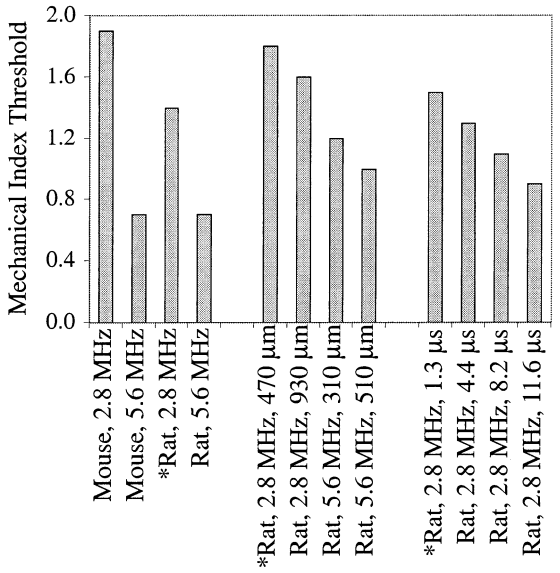

Fig. 3. The MI threshold in this study (right set of 4 bars) compared with that of two previous studies (left set of 4 bars, Zachary et al. 2001b; middle set of 4 bars, O'Brien et al. 2001a).

there was a significant trend. Because the PRF (1 kHz) and ED (10 s) were held constant, the total on-time and, thus, the temporal-average intensity, increased by a factor of 8.9 (11.6 μs/1.3 μs). But, near the ED_{05} occurrence and size threshold levels, the temporal-peak exposure quantities were about the same (2.0 to 3.1 MPa; with SEs around $\pm$ 0.6 MPa). This observation suggests that there is no need to consider a PD-dependency as part of an FDA or safety-based guideline that is based on US-induced lung hemorrhage.

However, the ED_{50} occurrence and size estimates (6.5 to 6.8 MPa and 5.3 to 5.5 MPa; with SEs around $\pm$ 0.3 MPa) for the two most extreme PDs (1.3 μs and 11.6 μs, respectively) were significant. This observation would suggest that either PD or a temporal-average exposure quantity may play a role in the mechanism responsible for US-induced lung hemorrhage.

The peak rarefactional pressure thresholds as a function of PD reported in mice (Child et al. 1990) were 1.4 MPa (PD = 1 μs) and 1.0 MPa (10 μs) at 3.7 MHz at PRF values of 100 Hz and 1 kHz, respectively. With two variables changing, it is not possible to determine which variable was the determinant one. In a factorial study (PRF $\times$ exposure duration or ED) conducted in mice and rats, the proportion of lesions in both species was related statistically to PRF and ED, with the exception that PRF in rats was not quite significant (O'Brien et al. 2001a). The results from this factorial study would suggest that a 100-Hz PRF would yield a lower peak rarefactional pressure threshold than a 1-kHz PRF; thus, suggesting that if the PD affected the peak rarefactional pressure threshold, so would the PRF in mice. Thus, the observations by Child et al. (1990) are inconclusive relative to a PD or PRF affect, and cannot be directly compared with the study reported herein.

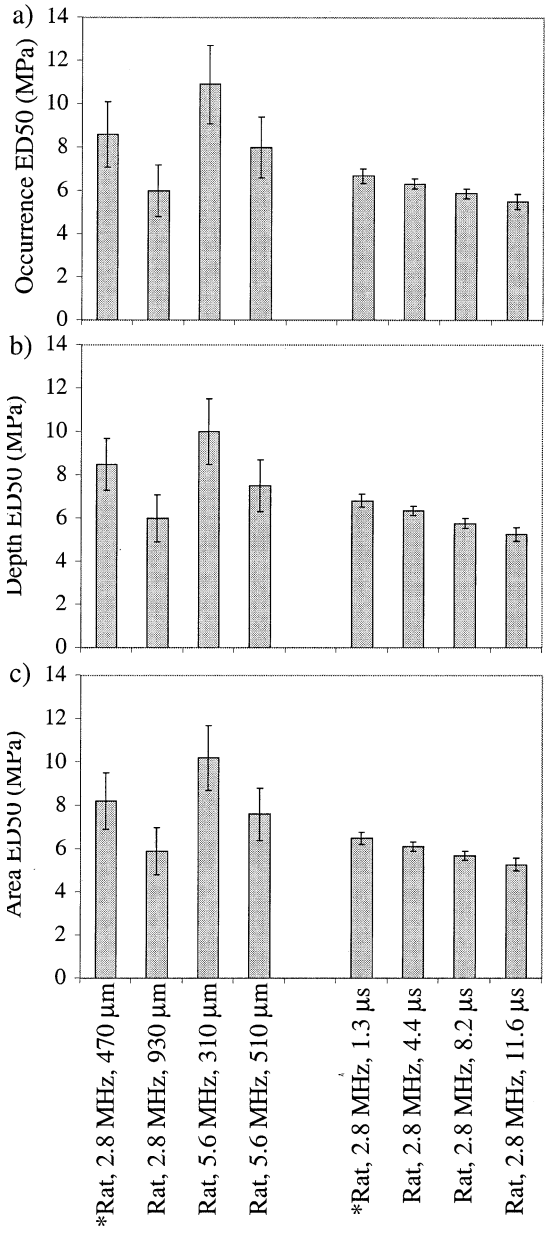

Fig. 4. The (a) lesion ED_{50} estimate occurrence, (b) lesion ED_{50} estimate depth, and (c) lesion ED_{50} estimate surface area in this study (right set of 4 bars), compared with a previous study (left set of 4 bars, O'Brien et al. 2001a).

Comparison of the ED_{05} threshold levels deduced herein with those of two previous studies (Zachary et al. 2001b; O'Brien et al. 2001a) suggests that the ED_{05} threshold levels are the same for lesion occurrence, depth and area (Fig. 2). Likewise, comparison of the ED_{50} superthreshold estimates deduced herein with those of another study (O'Brien et al. 2001b) suggests that the ED_{50} levels are the same for lesion occurrence, depth and area (Fig. 4). This level of agreement argues in favor of reproducible experimental procedures used in this study.

In summary, this study appears to be the first to report on the effects of US-induced lung damage as a function of PD for any species. Based on the overall exposure-effect observations, there appears to be a significant and monotonic effect for lesion occurrence, depth and area. However, the uncertainty is too great to determine if there is a significant ED_{05} threshold effect.

Acknowledgments—A special thanks to J. Blue, R. Miller and K. Norrell for conducting the experiments so reliably. The authors also thank J. Christoff, O. Coffield, T. Fong, B. McNeill, R. Patel, S. Sakai, R. Towa, A. Tevar and B. Zierfuss for technical assistance. This work was supported by NIH (grant EB02641; formerly HL58218) awarded to W.D. O'Brien Jr. and J.F. Zachary, and by NSF (grant DMS-0073044) awarded to D.G. Simpson.

REFERENCES

Agresti A. An introduction to categorical data analysis. New York: Wiley, 1996.

AIUM (American Institute of Ultrasound in Medicine). Mechanical bioeffects from diagnostic ultrasound: AIUM consensus statements. J Ultrasound Med 2000;19:67–168.

AIUM/NEMA (American Institute of Ultrasound in Medicine/National Electrical Manufacturers Association). Acoustic output measurement standard for diagnostic ultrasound equipment. Laurel, MD and Rosslyn, VA: AIUM/NEMA, 1998a.

AIUM/NEMA (American Institute of Ultrasound in Meidcine/National Electrical Manufacturers Association). ODS standard for real-time display of thermal and mechanical acoustic output indices on diagnostic ultrasound equipment, revision 1. Laurel, MD and Rosslyn, VA: AIUM/NEMA, 1998b.

Amemiya T. Tobit models: A survey. J Econometrics 1984;24:3–61.

Baggs R, Penney DP, Cox C, et al. Thresholds for ultrasonically induced lung hemorrhage in neonatal swine. Ultrasound Med Biol 1996;22:119–128.

Billard L. Presidential invited address: The world of biometry. Biometrics 1994;50:889–916.

Child SZ, Hartman CL, Schery LA, Carstensen EL. Lung damage from exposure to pulsed ultrasound. Ultrasound Med Biol 1990;16:817–825.

Dalecki D, Child SZ, Raeman CH, Cox C, Carstensen EL. Ultrasonically induced lung hemorrhage in young swine. Ultrasound Med Biol 1997a;23:777–781.

Dalecki D, Child SZ, Raeman CH, et al. Age-dependence of ultrasonically-induced lung hemorrhage in mice. Ultrasound Med Biol 1997b;23:767–776.

FDA (US Food and Drug Administration). Information for manufacturers seeking marketing clearance of diagnostic ultrasound systems and transducers. Rockville, MD: Center for Devices and Radiological Health, US FDA, 1997.

Frizzell LA, Chen E, Lee C. Effects of pulsed ultrasound on the mouse neonate: Hind limb paralysis and lung hemorrhage. Ultrasound Med Biol 1994;20:53–63.

Frizzell LA, O'Brien WD Jr, Zachary JF. Effect of pulse polarity and energy on ultrasound-induced lung hemorrhage in adult rats. J Acoust Soc Am 2003;113:2912–2926.

Galfalvy H, Simpson DG. Infrastructure degradation: An application of censored regression models. ASA Proceedings of the Section on Physical and Engineering Sciences 1999:242–247.

Hartman C, Child SZ, Mayer R, Schenk E, Carstensen EL. Lung damage from exposure to the fields of an electrohydraulic lithotripter. Ultrasound Med Biol 1990;16:675–683.

Holland CK, Deng CX, Apfel RE, et al. Direct evidence of cavitation *in vivo* from diagnostic ultrasound. Ultrasound Med Biol 1996;22: 917–925.

Kramer JM, Waldrop TG, Frizzell LA, Zachary JF, O'Brien WD Jr. Cardiopulmonary function in rats with lung hemorrhage induced by exposure to superthreshold pulsed ultrasound. J Ultrasound Med 2001;20:1197–1206.

O'Brien WD Jr, Zachary JF. Lung damage assessment from exposure to pulsed-wave ultrasound in the rabbit, mouse, and pig. IEEE Trans Ultrason Ferroelec Freq Control 1997;44:473–485.

O'Brien WD Jr, Frizzell LA, Schaeffer DJ, Zachary JF. Superthreshold behavior of ultrasound-induced lung hemorrhage in adult mice and rats: Role of pulse repetition frequency and pulse duration. Ultrasound Med Biol 2001a;27:267–277.

O'Brien WD Jr, Frizzell LA, Weigel RM, Zachary JF. Ultrasound-induced lung hemorrhage is not caused by inertial cavitation. J Acoust Soc Am 2000;108:1290–1297.

O'Brien WD Jr, Kramer JM, Waldrop TG, Frizzell LA, Zachary JF. Ultrasound-induced lung hemorrhage: Role of acoustic boundary conditions at the pleural surface. J Acoust Soc Am 2002;111:1102–1109.

O'Brien WD Jr, Simpson DG, Frizzell LA, Zachary JF. Superthreshold behavior and threshold estimation of ultrasound-induced lung hemorrhage in adult rats: Role of beamwidth. IEEE Trans Ultrason Ferroelec Freq Control 2001b;48:1695–1705.

O'Brien WD Jr, Simpson DG, Ho M-H, et al. Superthreshold behavior and threshold estimation of ultrasound-induced lung hemorrhage in pigs: Role of age dependency. IEEE Trans Ultrason Ferroelec Freq Control 2003;50:153–169.

Penney DP, Schenk EA, Maltby K, et al. Morphologic effects of pulsed ultrasound in the lung. Ultrasound Med Biol 1993;19:127–135.

Raeman CH, Child SZ, Carstensen EL. Timing of exposures in ultrasonic hemorrhage of murine lung. Ultrasound Med Biol 1993;19: 507–512.

Raeman CH, Child SZ, Dalecki D, Cox C, Carstensen EL. Exposure-time dependence of the threshold for ultrasonically induced murine lung hemorrhage. Ultrasound Med Biol 1996;22:139–141.

Raum K, O'Brien WD Jr. Pulse-echo field distribution measurement technique of high-frequency ultrasound sources. IEEE Trans Ultrason Ferroelec Freq Control 1997;44:810–815.

Sempsrott JM, O'Brien WD Jr. Experimental verification of acoustic saturation. Proceedings of the 1999 IEEE Ultrasonics Symposium. 1999:1287–1290.

Simpson DG, Carroll RJ, Zhou H, Guth DJ. Interval censoring and marginal analysis in ordinal regression. J Agric Biol Environm Stat 1996;1:354–376.

Tarantal AF, Canfield DR. Ultrasound-induced lung hemorrhage in the monkey. Ultrasound Med Biol 1994;20:65–72.

Teotico GA, Miller RJ, Frizzell LA, Zachary JF, O'Brien WD Jr. Attenuation coefficient estimates of mouse and rat chest wall. IEEE Trans Ultrason Ferroelec Freq Control 2001;48:593–601.

Towa RT, Miller RJ, Frizzell LA, Zachary JF, O'Brien WD Jr. Attenuation coefficient and propagation speed estimates of rat and pig

intercostal tissue as a function of temperature. IEEE Trans Ultrason Ferroelec Freq Control 2002;49:1411–1420.

Zachary JF, O'Brien WD Jr. Lung lesion induced by continuous- and pulsed-wave (diagnostic) ultrasound in mice, rabbits, and pigs. Vet Pathol 1995;32:43–45.

Zachary JF, Frizzell LA, Norrell KS, et al. Temporal and spatial evaluation of lesion resolution following exposure of rat lung to pulsed ultrasound. Ultrasound Med Biol 2001a;27:829–839.

Zachary JF, Sempsrott JM, Frizzell LA, Simpson DG, O'Brien WD Jr. Superthreshold behavior and threshold estimation of ultrasound-induced lung hemorrhage in adult mice and rats. IEEE Trans Ultrason Ferroelec Freq Control 2001b;48:581–592.